AIP Applied Physics Letters

Biosensor utilizing resist-derived carbon nanostructures

Jung A Lee, Seung S. Lee, Kwang-Cheol Lee, Se Il Park, Byung-Chill Woo et al.

Citation: Appl. Phys. Lett. **90**, 264103 (2007); doi: 10.1063/1.2752719
View online: http://dx.doi.org/10.1063/1.2752719
View Table of Contents: http://apl.aip.org/resource/1/APPLAB/v90/i26
Published by the American Institute of Physics.

Additional information on Appl. Phys. Lett.

Journal Homepage: http://apl.aip.org/
Journal Information: http://apl.aip.org/about/about_the_journal
Top downloads: http://apl.aip.org/features/most_downloaded
Information for Authors: http://apl.aip.org/authors

ADVERTISEMENT

Downloaded 21 Apr 2013 to 143.248.118.122. This article is copyrighted as indicated in the abstract. Reuse of AIP content is subject to the terms at: http://apl.aip.org/about/rights_and_permissions

Biosensor utilizing resist-derived carbon nanostructures

Jung A Lee and Seung S. Lee
Department of Mechanical Engineering, Korea Advanced Institute of Science and Technology, Daejeon 305-701, Korea

Kwang-Cheol Lee,[a] Se Il Park, and Byung-Chill Woo
Advanced Technology Division, Korea Research Institute of Standards and Science, Daejeon 305-340, Korea

Jeong-O Lee
Advanced Materials Division, Korea Research Institute of Chemical Technology, Daejeon 305-600, Korea

(Received 6 May 2007; accepted 29 May 2007; published online 27 June 2007)

The authors present a biosensor using pyrolyzed electron beam resist nanostructures as an active conducting channel. Versatile, arbitrarily shaped nanostructures such as nanowires, nanodots, and suspended nanobridges are fabricated by a facile electron beam resist thermal decomposition method. The nanostructures typically show 15–21 nm thickness, 100–200 nm width, 0.6 nm roughness, and *p*-type majority conduction with tailored resistivity of 5.2–0.75 Ω cm. Streptavidin-biotin binding and *p*H dependent conductance modulation are demonstrated using pyrolyzed resist based devices. © *2007 American Institute of Physics*. [DOI: 10.1063/1.2752719]

Detection of chemical or biological species using micro- or nanofabricated sensors is receiving great attention. In the case of mechanical sensors,[1–6] micro- or nanocantilever bending or resonance frequency changes are monitored by embedded piezoresistors, piezoelectric materials, or strain-sensitive field effect transistors (FETs). Electrical sensors for gas or biomolecule detection were demonstrated using semiconductor or polymer nanowires,[7–9] nanotubes,[10,11] and batch-fabricated silicon FETs.[12,13] Despite the apparent advantages of nanomaterial-based sensors, there are ongoing technological challenges such as assembly or chirality selection.[14,15] Low-cost batch fabrication of free-style, free-standing nanostructures can improve existing nanomaterial- and silicon-based devices and widen future nanotechnology applications.

Carbon thin film, which is fabricated by pyrolysis of patterned resist, shows amorphous, graphitelike characteristics with tunable conductivity versus pyrolysis temperatures.[16–18] Because the carbon film is fabricated through lithography processes, we can obtain free-handed micro- or nanostructures on a silicon substrate, where the feature size is limited by top-down lithography techniques. While electrochemical behaviors and applications such as microbatteries, molecular electronics, and image sensors are extensively studied, mechanical and electrical property utilizations, especially overhanging nanostructures for sensor and actuator applications, are rarely reported.[19–21]

In this letter, we present fabrication of versatile carbon nanostructures derived from electron beam resist for various sensor and actuator applications and their utilization in biosensors. Various resist shapes, including nanowires, nanodots, and wheels, were patterned using a negative electron beam resist SAL-601 (Shipley Co.), and a modified scanning electron microscope (JSM-6400, JEOL). Nanoscale carbon mechanical structures are fabricated by pyrolysis of the electron beam resist pattern and sacrificial oxide etching.

Figure 1 shows an example of fabrication processes for nanoscale carbon devices. The fabrication process starts with 0.8-μm-thick SiO_2 growing by thermal oxidation onto a 4 in. Si P (100) wafer [Fig. 1(a)]. A 70-nm-thick Au layer over a 10-nm-thick Cr layer, for align markers for electron beam lithography and metal pads, was delineated using lift-off technique [Fig. 1(b)]. Electron beam resist patterns were fabricated through exposures at 30 keV energy, 1 $\mu C/cm^2$ dose, and development with AZ300MIF for 5 min [Fig. 1(c)].

The resist pattern was converted to an amorphous carbon phase by pyrolysis [Fig. 1(d)]. The thickness of the carbon

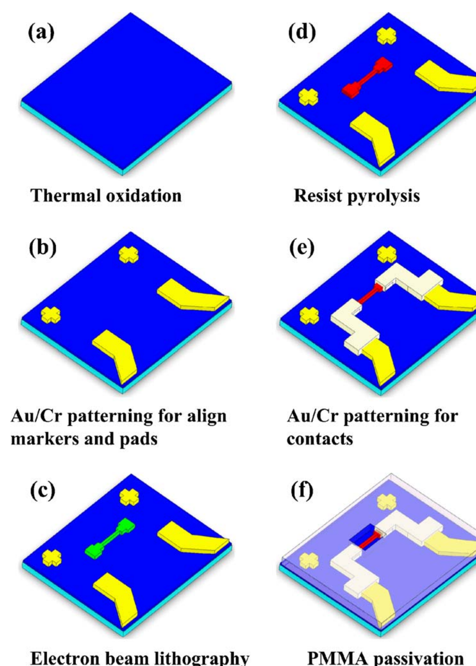

FIG. 1. (Color online) Fabrication processes of nano carbon devices: (a) thermal oxidation for diffusion barrier and isolation, (b) electrode patterning for alignment and pads, (c) resist patterning by electron beam lithography, (d) resist pyrolysis to obtain carbon nanopatterns, (e) connecting carbon to pads, and (f) passivation with PMMA against electrolytes or for releasing carbon mechanical nanodevices.

[a]Electronic mail: kclee@kriss.re.kr

 © 2007 American Institute of Physics

Downloaded 21 Apr 2013 to 143.248.118.122. This article is copyrighted as indicated in the abstract. Reuse of AIP content is subject to the terms at: http://apl.aip.org/about/rights_and_permissions

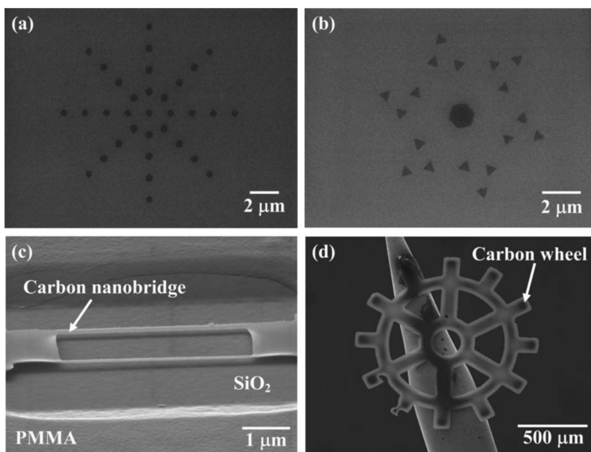

FIG. 2. Scanning electron microscopy (SEM) photomicrographs of carbon structures fabricated from resists: (a) 250-nm-radius circular dots, (b) triangles on silicon substrates, (c) 130-nm-wide, 15-nm-thick, 4-μm-long carbon nanobridges suspended from silicon substrate, and (d) a 1-μm-thick microwheel on a tungsten needle. [A negative electron beam resist, SAL-601, is used for (a)–(c). A positive photoresist, AZ9260, is used for (d).]

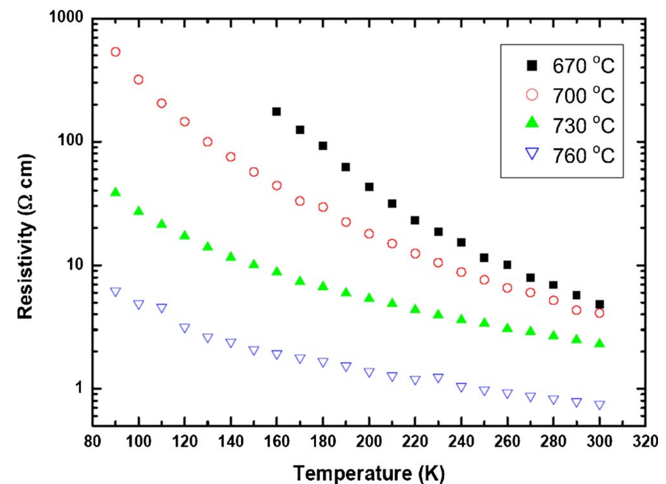

FIG. 3. (Color online) Resistivity variations vs temperature for carbon films pyrolyzed between 670 and 760 °C. Carbon resistivity was measured by the van der Pauw method with a Greek cross test pattern. Measured resistivity was fitted to a formula, $\rho(T)=\rho_0 \exp[(T_0/T)^{1/4}]$. In the case of films pyrolyzed at 700 °C, ρ_0 of 3.8×10^{-6} Ω cm and hopping barrier T_0 of 1.1×10^{7} K were obtained.

layer obtained after pyrolysis was between 15 and 21 nm, which was 16%–25% of the initial resist thickness of 80–110 nm. Resistivity of the carbon layer was between 5.2 and 0.75 Ω cm and decreased as pyrolysis temperature increased.

Carbon nanopatterns were connected to source and drain electrodes via the Au/Cr layer through electron beam lithography and lift-off technique [Fig. 1(e)]. Polymethyl methacrylate (PMMA) passivation followed in order to shield metal electrodes from liquids [Fig. 1(f)]. Suspended carbon mechanical nanostructures were fabricated by etching underlying the oxide layer using buffered HF.

Various carbon micro- and nanostructures, such as nanowires, nanodots, and nanochannels, were fabricated using this method (Fig. 2). Double-clamped carbon nanobridges [130 nm wide, 15 nm thick, and 4 μm long, as shown in Fig. 2(c)] were fabricated by oxide etching with buffered HF for 3 min. The carbon nanobridges can be used as resonant sensors for minuscule force or mass detection. Suspended nanobridges, which have a larger surface-to-volume ratio (a factor of 2) compared to nanowires with similar dimensions, will be useful for surface-sensitive devices such as gas sensors and biosensors. Figure 2(d) shows a carbon microwheel on a tungsten needle, fabricated from 5-μm-thick AZ9260 photoresist, which is separated from the silicon substrate by underlying oxide etching. Floating micro- or nanocarbon devices, such as those in Fig. 2(d), have advantages such as batch-fabrication and mass production without etch and deposition processes, and also have potential applications such as actuators, nanodust, and self-propelling nanorobots.[22]

Figure 3 shows resistivity variations according to temperature for films pyrolyzed between 670 and 760 °C. Carbon resistivity, $\rho(T)$, decreased monotonically as temperature T increased between 90 and 300 K. We used the formula, $\rho(T)=\rho_0 \exp[(T_0/T)^{1/4}]$,[23] to fit the resistivity data. For films pyrolyzed at 700 °C, a ρ_0 of 3.8×10^{-6} Ω cm and a hopping barrier T_0 of 1.1×10^{7} K were obtained. Black, opaque, smooth carbon surfaces, with root mean square roughness below 0.6 nm and indistinguishable top and bottom sides, were obtained using mirror-polished silicon substrates and slow out-gassing during heat treatment. For carbon films pyrolyzed at 700 °C, a weak p-type majority conduction carrier with Hall coefficient of 0.44 cm^3/C was measured.

Many promising applications for nanoscale devices, such as thermistors, heaters, and interconnects, are anticipated using the mechanical and electrical properties of resist-derived carbon nanostructures. Next, we studied applications of carbon nanostructures to active channels in electrical biosensors. For biosensing applications, we used carbon films pyrolyzed at 700 °C because of the medium conductivity of a few Ω cm and to avoid excess carrier density. Streptavidin (Sigma), which has high binding affinity to biotin, was employed as a model protein. Carbon biosensors [Fig. 4(a)] were fabricated using the processes shown in Fig. 1. After PMMA passivation, as shown in Fig. 1(f), O_2 plasma treatment at 150 mTorr and 50 W for 15 s was carried out to increase the density of the oxygen-containing functional groups.

The devices were incubated in 100 μl ethanol with 50 mM 1-ethyl-3-(3-dimethylaminopropyl) carbodiimide hydrochloride (EDC) (Aldrich) and 50 mM N-hydroxysuccinimide (NHS) (Aldrich) for 2 h and were then rinsed with ethanol. The devices were kept in 100 μl ethanol with 1 mg/ml amine-conjugated biotin for 2 h and were then rinsed thoroughly with ethanol and phosphate buffered saline (PBS) (pH 7.4, Bioneer Co., Korea), respectively. The carboxyl (COOH) groups on the carbon surface were transformed using EDC/NHS into intermediates that readily react with the NH_2 groups on biotin. The biotin was immobilized onto the carbon surface using an amide bond.

Figure 4(b) shows measurements of source-to-drain current I_{DS} versus time for V_{DS}=300 mV after introduction of 0.5 mg/ml streptavidin in 10 mM PBS solution (pH 7.4). Whereas I_{DS} for the biotin-unmodified control device was not changed after streptavidin injection [inset in Fig. 4(b)], we observed increases in I_{DS} for the biotin-treated device after streptavidin introduction. Carbon devices after streptavidin injection also showed pH sensitivity, with increases in I_{DS} with pH, as shown in Fig. 4(c). For negative gate voltage ($V_{GS}<0$), the drain current I_{DS} for carbon devices after

Downloaded 21 Apr 2013 to 143.248.118.122. This article is copyrighted as indicated in the abstract. Reuse of AIP content is subject to the terms at: http://apl.aip.org/about/rights_and_permissions

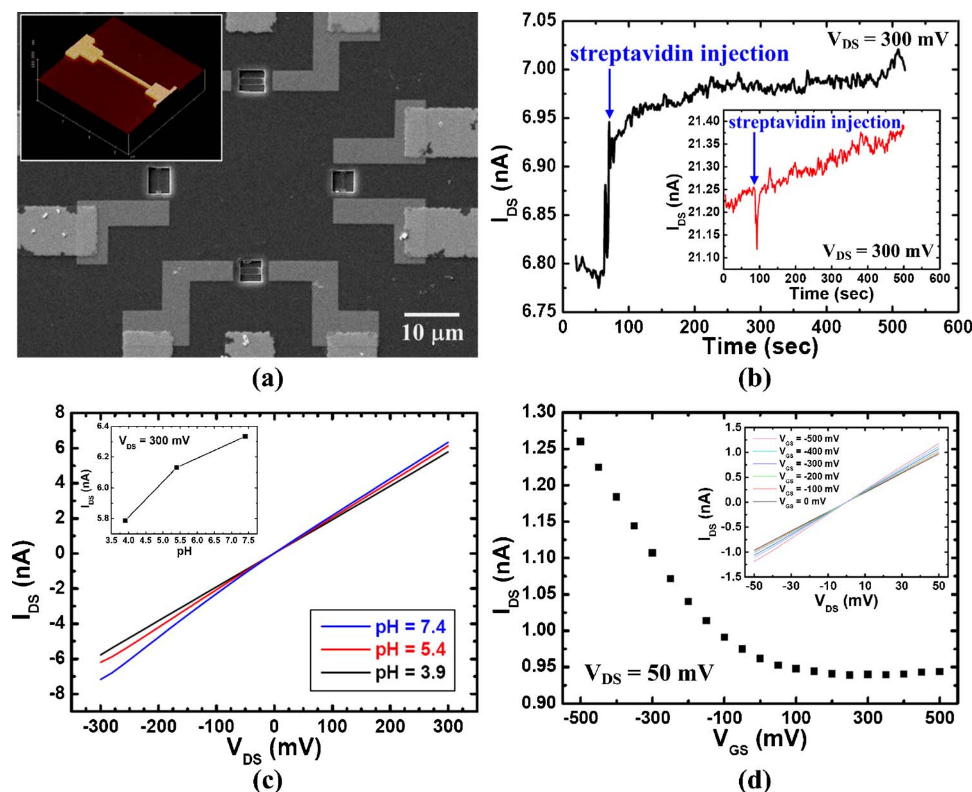

FIG. 4. (Color online) (a) SEM photomicrograph of a fabricated carbon nanobiosensor (inset: AFM image of a carbon channel), (b) source-to-drain current I_{DS}, vs time after streptavidin injection onto biotin-grafted device (V_{DS}=300 mV, ↓: streptavidin injection) (inset: a control experiment onto biotin-untreated device), (c) I_{DS}-V_{DS} curves showing *p*H sensitivity for the device covered with streptavidin/biotin where I_{DS} increases as *p*H increases (inset: I_{DS} vs *p*H), (d) I_{DS} vs gate voltage, V_{GS}, for the device covered with streptavidin/biotin (V_{DS}=50 mV). For $V_{GS}<0$, I_{DS} increases as V_{GS} decreases (inset: I_{DS}-V_{DS} curves vs V_{GS}).

streptavidin injection increases as gate voltage V_{GS} decreases, as shown in Fig. 4(d).

In summary, we demonstrated fabrication, using a facile electron beam resist pyrolysis method, of arbitrarily shaped, freestanding carbon nanostructures for various sensors and actuators applications. The nanofabrication method, based on lithography and thermal processes, eliminates additional processes such as reactive ion etching and provides batch-fabricated, low-cost nanodevices. We also studied biosensing applications of carbon nanostructures for a potential low-cost point-of-care testing tool. We expect that the carbon nanostructures, fabricated from combinations of resist pyrolysis and nanomachining processes, will provide a method for nanofabrication in NEMS and nanodevices.

This work was supported by the Brain Korea 21 program and the National Nano Program for Applications (KOSEF 2006-04921).

[1]G. Wu, H. Ji, K. Hansen, T. Thundat, R. Datar, R. Cote, M. F. Hagan, A. K. Chakraborty, and A. Majumdar, Proc. Natl. Acad. Sci. U.S.A. **98**, 1560 (2001).
[2]J. Fritz, M. K. Baller, H. P. Lang, H. Rothuizen, P. Vettiger, E. Meyer, H.-J. Güntherodt, Ch. Gerber, and J. K. Gimzewski, Science **288**, 316 (2000).
[3]N. V. Lavrik, M. J. Sepaniak, and P. G. Datskos, Rev. Sci. Instrum. **75**, 2230 (2004).
[4]G. Abadal, Z. J. Davis, B. Helbo, X. Borrisé, R. Ruiz, A. Boisen, F. Campabadal, J. Esteve, E. Figueras, F. Pérez-Murano, and N. Barniol, Nanotechnology **12**, 100 (2001).
[5]G. Shekhawat, S.-H. Tark, and V. P. Dravid, Science **311**, 1592 (2006).
[6]P. A. Truitt, J. B. Hertzberg, C. C. Huang, K. L. Ekinci, and K. C. Schwab, Nano Lett. **7**, 120 (2007).
[7]J. Hahm and C. M. Lieber, Nano Lett. **4**, 51 (2004).
[8]K. Ramanathan, M. A. Bangar, M. Yun, W. Chen, N. V. Myung, and A. Mulchandani, J. Am. Chem. Soc. **127**, 496 (2005).
[9]H. Liu, J. Kameoka, D. A. Czaplewski, and H. G. Craighead, Nano Lett. **4**, 671 (2004).
[10]J. Kong, N. R. Franklin, C. Zhou, M. G. Chapline, S. Peng, K. Cho, and H. Dai, Science **287**, 622 (2000).
[11]H.-M. So, K. Won, Y. H. Kim, B.-K. Kim, B. H. Ryu, P. S. Na, H. Kim, and J.-O. Lee, J. Am. Chem. Soc. **127**, 11906 (2005).
[12]Z. Li, Y. Chen, X. Li, T. I. Kamins, K. Nauka, and R. S. Williams, Nano Lett. **4**, 245 (2004).
[13]S.-M. Koo, Q. Li, M. D. Edelstein, C. A. Richter, and E. M. Vogel, Nano Lett. **5**, 2519 (2005).
[14]P. A. Smith, C. D. Nordquist, T. N. Jackson, T. S. Mayer, B. R. Martin, J. Mbindyo, and T. E. Mallouk, Appl. Phys. Lett. **77**, 1399 (2000).
[15]Y. Huang, X. Duan, Y. Cui, L. J. Lauhon, K. Kim, and C. M. Lieber, Science **294**, 1313 (2001).
[16]R. Kostecki, B. Schnyder, D. Alliata, X. Song, K. Kinoshita, and R. Kötz, Thin Solid Films **396**, 36 (2001).
[17]J. Kim, X. Song, K. Kinoshita, M. Madou, and R. White, J. Electrochem. Soc. **145**, 2314 (1998).
[18]N. E. Hebert, B. Snyder, R. L. McCreery, W. G. Kuhr, and S. A. Brazill, Anal. Chem. **75**, 4265 (2003).
[19]O. J. A. Schueller, S. T. Brittain, and G. M. Whitesides, Sens. Actuators, A **72**, 125 (1999).
[20]S. Ranganathan, I. Steidel, F. Anariba, and R. L. McCreery, Nano Lett. **1**, 491 (2001).
[21]C. Wang, G. Jia, L. H. Taherabadi, and M. J. Madou, J. Microelectromech. Syst. **14**, 348 (2005).
[22]P. Dhar, Th. M. Fischer, Y. Wang, T. E. Mallouk, W. F. Paxton, and A. Sen, Nano Lett. **6**, 66 (2006).
[23]N. F. Mott and E. A. Davis, *Electronic Processes in Non-Crystalline Materials* (Clarendon, Oxford, 1979), pp. 7–64.

Downloaded 21 Apr 2013 to 143.248.118.122. This article is copyrighted as indicated in the abstract. Reuse of AIP content is subject to the terms at: http://apl.aip.org/about/rights_and_permissions